

Benchmarking of Deep Reinforcement Learning Algorithms for Vision-based Robotics

Swagat Kumar, Hayden Sampson and Ardhendu Behera

Abstract—This paper presents a benchmarking study of some of the state-of-the-art reinforcement learning algorithms used for solving two simulated vision-based robotics problems. The algorithms considered in this study include soft actor-critic (SAC), proximal policy optimization (PPO), interpolated policy gradients (IPG), and their variants with Hindsight Experience replay (HER). The performances of these algorithms are compared against PyBullet’s two simulation environments known as KukaDiverseObjectEnv and RacecarZEDGymEnv respectively. The state observations in these environments are available in the form of RGB images and the action space is continuous, making them difficult to solve. A number of strategies are suggested to provide intermediate hindsight goals required for implementing HER algorithm on these problems which are essentially single-goal environments. In addition, a number of feature extraction architectures are proposed to incorporate spatial and temporal attention in the learning process. Through rigorous simulation experiments, the improvement achieved with these components are established. To the best of our knowledge, such a benchmarking study is not available for the above two vision-based robotics problems making it a novel contribution in the field.

I. INTRODUCTION

Vision-based Robots use visual feedback to guide their motion. The underlying problem, also known as hand-eye coordination [17] or visual servoing [7], is considered to be difficult due to factors such as non-linearity and uncertainty of camera and robot models, sensor noise, mathematical complexity of extracting geometrical features from images and difficulty in deriving closed-form analytical control equations in terms of these image features etc. Traditional model-based methods addressed some of these concerns by adopting soft computing approaches [46] [24] [11]. The recent success of deep learning methods in computer vision has greatly enhanced the capabilities of these model-based methods [5] [40] [26] [27]. In contrast, reinforcement learning (RL) offers a model-free alternative to solve this problem directly from input-output data, thereby overcoming many of the above problems. It has the potential to create truly autonomous agents that can learn skills on its own without needing human intervention. An RL agent learns the desired behaviour, over time, through trial and error while repeatedly interacting with its environment [47]. The agent achieves this by taking actions to maximize the *cumulative discounted future reward* for a given task while balancing *exploration* (of new possibilities) and *exploitation* (of past experiences). This cumulative discounted reward function, represented as

Q or value function, is used to evaluate a given action, and is not known a priori. Depending on how this function is estimated and desirable actions are derived from it, the RL-based methods can be broadly classified into two categories: *value-based* methods and *policy-based* methods. Value-based methods aim at estimating the Q-function and then derive action from this by using a greedy policy. On the other hand, policy-based methods directly estimate the policy function by maximizing a given objective function. The traditional Q-learning algorithm estimates the Q function iteratively by using an approximate dynamic programming formulation based on Bellman’s equation starting from an initial estimate [4]. The original Q-learning algorithm could be applied to problems with discrete state (observation) and action spaces, and suffer from the *curse-of-dimensionality* problem with higher dimensions and range of values. This limitation can be overcome by using a deep network to estimate Q function from arbitrary observation inputs, thereby, greatly enhancing the capabilities of RL algorithms. The resulting approach is known as Deep Q Networks (DQN) [48] [45] which has been applied successfully to a wide range of problems while achieving superhuman level performances in a few cases, such as ATARI video games [32], Go [18] etc. The success of DQN has spawned a new research field known as deep reinforcement learning (DRL) attracting a large following of researchers. Readers are referred to [2] for a survey of this field. The DQN models were subsequently extended to continuous action spaces by using policy gradient methods that used a parameterized policy function to maximize DQN output using gradient ascent methods [28] [9]. This has opened the doors for solving various robotics problems that use continuous values such as joint angle, joint velocities or motor torques as input. Since then, a number of methods have been proposed to improve the performance of RL algorithms and have been applied successfully to different robotic problems - manipulation [14] [34], grasping [38] [20], navigation [50] etc.

Since RL algorithms vary greatly in terms of model complexity, choice of hyper-parameters and architectures, it becomes necessary to benchmark them against standard problems to assess their performances. One such effort was made for a robotic grasp problem in [38] where authors compared the performance of three off-policy methods including DDPG [28] on a simulated Kuka environment created using PyBullet [37]. A similar benchmarking was done for continuous control problems in [9] where authors compared the performance of several off-policy and on-policy methods on several simulated environments created using MuJoCo

The authors are with the department of Computer Science, Edge Hill University, Ormskirk, UK L39 4QP. email: {kumars, haydens, beheraa}@edgehill.ac.uk.

[33]. A benchmarking of reinforcement learning algorithms on real-world robots was carried out in [30] that included algorithms such as TRPO [41] and PPO [43].

The focus of this paper is to benchmark some of the newer deep reinforcement learning algorithms such as Soft Actor Critic (SAC) [16], Proximal Policy Optimization (PPO) [43] and Interpolated Policy Gradients (IPG) [15] for solving vision-based robotic problems in an end-to-end fashion. The problems used for this study include two PyBullet [37] simulation environment, namely, `KukaDiverseObject` and `RacecarZEDGym`. Both environments provide observations in the form of RGB images and take continuous action inputs which makes these two problems more difficult compared to the versions where observations are available as floating point vectors. We then demonstrate that the performance of these algorithms can be further improved by using Hindsight experience replay (HER) [1] where the problem of sparse rewards is partially addressed by providing intermediate goals. HER is shown to be more effective for multi-goal problems such as MuJoCo’s Fetch environment [35] or PyBullet’s Panda robot [12]. Both of these two environments do not provide image observations making them unsuitable for this study. A number of strategies are proposed to provide intermediate goals for the above two environments to facilitate implementation of HER algorithm and show improvement in performance achieved. Finally, a number of architectures are presented to incorporate spatial and temporal attention into the learning process. Attention mechanisms [49] have been shown to improve the inference capability of a model by focussing on relevant parts and ignoring the irrelevant parts of the input observation. While the application of attention in reinforcement learning is not new, it has not been applied to the context of vision-based robotics problems considered in this paper. The performance improvement achieved by incorporating these concepts are demonstrated through rigorous simulation experiments which will be discussed later in this paper.

In short, the novel contributions made in this paper are as follows:

- A benchmarking of three RL algorithms, namely, SAC, PPO, IPG and their corresponding HER-variants have been carried out for two simulated vision-based robotics problem. This is the first-time such an effort has been made for these two simulated PyBullet environments.
- Several strategies are proposed to implement HER algorithm on these two environments which are essentially single-goal problems and do not provide intermediate goals. These ideas could be easily applied to other single-goal environments thereby extending the applicability of HER algorithms.
- Several architectures are proposed for incorporating spatial and temporal attention during the feature extraction process leading to improved learning performance. Through experiments, it is established that stacked frames along with attention and LSTM layers can provide superior learning performance. The application of attention in the present context of vision-based robotics

is new and has not been reported so far.

The rest of this paper is organized as follows. The details of RL model architectures, algorithms and methods are discussed in Section III. The details of experiments and analysis of results are presented in Section IV. The conclusion and direction of future research is provided in Section V.

II. PROBLEM ENVIRONMENTS

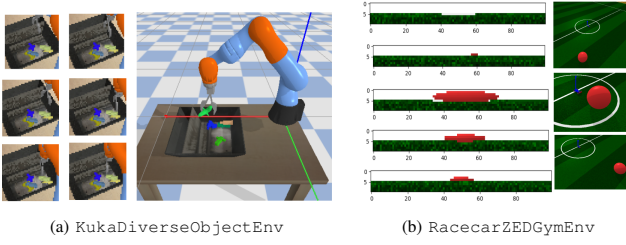
The objective of this work is to benchmark a few deep reinforcement learning algorithms, namely, soft actor critic (SAC) [16], proximal policy optimization (PPO) [43], interpolated policy gradients (IPG) [15] and hindsight experience replay (HER) [1] on two vision-based robotics problem. The data intensive nature of reinforcement learning necessitates use of simulated environments for training models. Two PyBullet [37] environments namely `KukaDiverseObjectEnv` and `RacecarZEDGymEnv` are used for implementing different RL algorithms. In the first environment, a Kuka robotic arm is used to grasp different kinds of objects from a bin. The environment gives a reward of 1 when one of the objects is picked up beyond a pre-defined height. The maximum reward for a given episode is 1 for the kuka environment. The second environment consists of a robotic car in a stadium and it is expected to reach a given target ball location by generating linear and angular velocities. The agent receives a floating point reward for each step in the episode. The input observation for both environments is available in the form of RGB images and the system accepts continuous floating point values as actions. A snapshot of the environment rendering and corresponding variables are shown in Figure 1. These two environments are selected as they are freely available and fall within the scope of vision-based robotics which is the focus of this work. Our algorithms work equally well with other environments such as `FetchReach` from Mujoco [33]. However, the results have not been included in this study because of two reasons - first, they are proprietary and require purchasing license for long-term use and secondly, image observations are not available for this environment.

III. METHOD

This section provides the details of models, architectures and algorithms used for this benchmarking study as described in the following subsections.

A. The RL formulation

An RL agent in state $s_t = s$ at time t takes an action $a_t = a$ according to its policy $\pi(a|s)$. The state transitions to state $s_{t+1} = s'$ at $t + 1$ while receiving a reward $r(s_t, a_t) = r$ from the environment. The terminal state of an episode is represented by a boolean variable d . The goal of the reinforcement learning is to learn a policy that will maximize the discounted cumulative future returns given by $J(\theta) = \mathbb{E}_{s, a \sim \pi} [\sum_{t=0}^{\infty} \gamma^t r(s_t, a_t)]$ where γ is the discount factor. This RL problem is solved in this paper using an actor-critic model [13] [23] that uses two different deep networks - an actor network for learning the policy function $\pi_{\theta}(a|s)$



Parameters	KukaDiverseObjectEnv	RacecarZEDGymENV
Observation shape s	(48, 48, 3)	(10, 100, 4)
Action a	(3,)	(2,)
Action Range	[-1, 1]	[-1, 1]
Reward Range r	(-inf, inf)	(-inf, inf)
Max steps / episode	20	100

(c) Environment parameters

Fig. 1: PyBullet Simulation Environment used for benchmarking RL algorithms. The input observation is available in the form of RGB images and the action input are continuous floating point values. The images for the racecar environment are resized to (40,40,3) before use.

and a critic network for estimating the value function $V_w(s)$ or the Q-function $Q_w(s, a)$ where θ and w are the trainable parameters. The critic is trained to minimize the time-delay (TD) error function (also known as mean square Bellman error (MSBE)) given by:

$$L(w_t) = \mathbb{E}[y - Q(s, a; w_t)] \quad (1)$$

where the target signal y is obtained from the recursive Bellman's equation given by:

$$y = \mathbb{E}_{s' \in S} [r + \gamma \max_{a' \in \pi(s')} Q(s', a'; w_{t-1})] \quad (2)$$

The training process for critic network is similar to that of DQN [32] that uses off-policy experience replay to improve the sample efficiency. The experience tuples (s, a, r, s', d) are stored in a replay buffer \mathcal{B} and then sampled in mini-batches during the training process. The actor network, on the other hand, is trained using a policy gradient method where the model parameters θ are updated so as to maximize the critic output. For instance, DDPG [28] optimize a continuous deterministic policy $\pi_\theta(a_t|s_t) = \delta(a_t = \mu_\theta(s_t))$ by applying the gradient ascent to the critic output directly as shown below:

$$\theta \leftarrow \theta + \alpha \mathbb{E}_{s, \pi \sim \mathcal{B}} [\nabla_\theta Q_w(s, \mu_\theta(s))] \quad (3)$$

where α is the learning rate. DDPG uses target networks to stabilize the learning process which are updated at a slower rate compared to original models by using Polyak averaging [36]. DDPG is known to be sensitive to the choices of parameters and sometimes overestimates Q-values. This is remedied in Twin-delayed DDPG (TD3) algorithm [8] that uses clipped double-Q learning, delayed policy updates and target policy smoothing to improve the learning performance. Many other on-policy and off-policy methods have been reported in literature to provide superior learning performances. Some of these methods are briefly discussed in the following subsections.

B. Model Architecture

An overview of actor-critic model used in this paper is shown in Figure 2. It consists of an actor network and a critic network. The actor network approximates the policy function required for producing actions for a given state observation. The critic network, on the other hand, evaluates the actor network by estimating the value function $V(s)$ or the Q function $Q(s, a)$. Both of these networks share a common

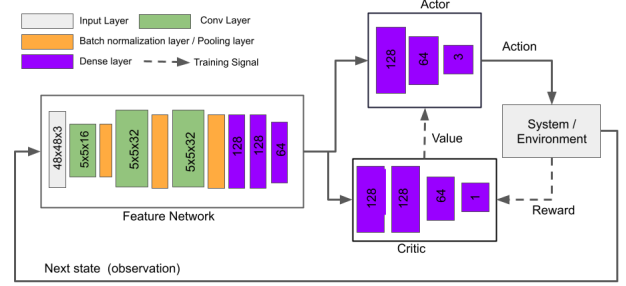


Fig. 2: Actor-Critic Architecture used for implementing RL algorithms. The feature network is shared by both actor and critic models. Actor network approximates the policy function required for producing actions required for transitioning to next states. The state observations are made available in the form of RGB images. Critic estimates value function $V(s)$ or Q-function $Q(s, a)$.

feature network which is used for extracting features from the input RGB images. The feature network is essentially a convolutional neural network (CNN). The number and size of convolutional and dense layers may vary from problem to problem. The feature network may include attention layers, and LSTM layers if required as will be discussed later in this paper. It may also be configured to receive a single image or a stack of frames as input. The RL algorithms used for solving the above problem is described next in this section.

C. Soft Actor-Critic Algorithm

Soft Actor Critic (SAC) [16] algorithm optimizes a stochastic policy in an off-policy manner. It uses a concept called entropy regularization where the policy is trained to maximize a trade-off between expected return and entropy in the policy. In addition, it borrows clipped double-Q trick from TD3 for stabilizing the training process. The target signal needed for critic update is given by

$$y = r + \gamma(1 - d) \left(\min_{i=1,2} Q_{\text{target},i}(s', a') - \alpha \log \pi_\theta(a'|s') \right)$$

where the action values a' are sampled from the current policy $\pi_\theta(\cdot|s)$. Hence, the critic is trained by using gradient-descent to minimize the MSBE equation (1) over mini-batches sampled from the replay buffer. The policy parameters are updated by applying gradient-ascent to maximize

the entropy-regularized value function. The corresponding gradient term may be written as follows:

$$\nabla_{\theta} \frac{1}{|\mathcal{B}|} \sum_{s \in \mathcal{B}} \left(\min_{i=1,2} Q_{w_i}(s, \tilde{a}_{\theta}(s)) - \alpha \log \pi_{\theta}(\tilde{a}_{\theta}(s)|s) \right)$$

where $\tilde{a}_{\theta}(s)$ is a sample from $\pi_{\theta}(\cdot|s)$ which is differentiable with respect to θ .

D. Proximal Policy Optimization

On-policy methods use the likelihood ratio policy gradient given below for policy optimization:

$$\nabla_{\theta} J(\theta) = \mathbb{E}[\nabla_{\theta} \log \pi_{\theta}(a|s) \hat{A}(s, a)] \quad (4)$$

where $\hat{A}(s, a)$ is the estimate of advantage function. Proximal Policy Optimization (PPO) [43], like its predecessor TRPO [41], tries to maximize the policy improvement step while keeping the new policy close to the old policy. It simplifies the TRPO by using a clipped version of objective function which is much easier to implement. The policy update equation is given by:

$$\theta_{k+1} = \arg \max_{\theta} \frac{1}{|\mathcal{D}_k|T} \sum_{\tau \in \mathcal{D}_k} \sum_{t=0}^T \min \left(\frac{\pi_{\theta}(a_t|s_t)}{\pi_{\theta_k}(a_t|s_t)} A^{\pi_{\theta_k}}(s_t, a_t), g(\epsilon, A^{\pi_{\theta_k}}(s_t, a_t)) \right) \quad (5)$$

where

$$g(\epsilon, A) = \begin{cases} (1 + \epsilon)A, & A > 0 \\ (1 - \epsilon)A, & A < 0 \end{cases}$$

is the clipped advantage function used to constrain the new policy. $\hat{A} = A^{\pi_{\theta}}$ is the generalized advantage estimate (GAE) [42] obtained from the current trajectories stored in an on-policy buffer \mathcal{D}_k . The critic uses a gradient descent algorithm to minimize the mean square Bellman error (MSBE) as described before. Compared to off-policy methods, on-policy gradient methods tend to be stable and relatively easier to implement. However, on-policy methods are known to be highly data inefficient as they look into the data only once.

E. Interpolated Policy Gradient

Interpolated policy gradient (IPG) [15] combines the benefits of both off-policy and on-policy algorithms to provide superior learning performance. Specifically, it mixes likelihood ratio gradient \hat{Q} and deterministic gradient through an off-policy fitted critic Q_w . It uses the parameter ν to trade-off bias and variance directly and a control variate to further reduce the estimator variance. The overall policy gradient can be written as:

$$\nabla_{\theta} J(\theta) \approx (1 - \nu) \mathbb{E}_{\rho^{\pi, \pi}} [\nabla_{\theta} \log \pi_{\theta}(a_t|s_t) (\hat{A}(s_t, a_t) - A_w^{\pi}(s_t, a_t))] + \mathbb{E}_{\rho^{\beta}} [\nabla_{\theta} \bar{Q}_w^{\pi}(s_t)] \quad (6)$$

where ρ^{β} refers to off-policy state sampling and ρ^{π} refers to on-policy state sampling. $A_w^{\pi}(s_t, a_t)$ is the advantage estimated with a baseline value function estimator which acts as a control variate to reduce the overall variance of the policy estimator.

F. Hindsight Experience Replay

Hindsight experience replay (HER) [1] solves the sparse reward problem in RL by providing positive reward even for failed states. In other words, it is motivated by the human ability to learn useful things from failed attempts. Usually, HER is applied to multi-goal environments where the agent is provided with intermediate goals to achieve. Existing multi-goal environments such as Mujoco’s FetchReach-v1 [10] and PyBullet’s Panda-Gym [12] do not provide image observations which is necessitated by the scope of this study. Hence, we propose three strategies to provide intermediate goals for the problem environments considered in this paper. The first one is the ‘success’ strategy where the hindsight goal (g^h) is selected randomly from a buffer containing previously encountered successful next states ($g^h = s' : r = 1$). The second strategy is called ‘final’ state strategy that uses the next state of the terminal step of the episode ($g^h = s' : d = 1$) as the hindsight goal. The third strategy is called ‘future’ state strategy where the hindsight goal is selected randomly from future steps of the current buffer ($g_i^h = s'_k : i < k < n, n = |\mathcal{B}|$). The agent receives an intermediate reward of 1 when the L2-norm of distance between the current next state and hindsight goal is less than a user-defined threshold. Instead of calculating L2-distance directly between the images, it is possible to compute the distance between the extracted features. This is denoted by an additional letter ‘F’ in the names used for labelling the plots. Mathematically, the hindsight reward for a given time step i is given by:

$$r_i^h = \begin{cases} 1 & \text{if } \|g_i^h - s'_i\| < h \\ 0 & \text{otherwise} \end{cases} \quad (7)$$

where h is an user-defined threshold which kept at a value of 0.3 in this paper. The implemented HER strategies is shown to provide improvement over the IPG algorithm.

G. Attention Architectures

As mentioned earlier, attention allows models to focus on task-relevant aspects of the observations thereby providing robustness against distractions and increased learning efficiency [49] [22]. The use of attention mechanisms have been shown to improve the performance of deep reinforcement learning algorithms [31]. For instance, authors in [31] have suggested several attention mechanisms to improve RL performance in solving Arcade video games. Similarly, authors in [39] use attention layers along with privileged information (environment states) to improve RL performance. Authors in [19] have used attention along with an actor-critic model to solve a multi-agent RL problem.

In this paper, we apply attention to two vision-based robotics problems. Two types of attention mechanisms, namely, Bahdanau’s additive type [3] and Luong’s dot product type [29] are used in four different configuration as shown in Figure 3. The attention layers are used within a feature network which is shared by both actor and critic models. An optional LSTM layer is also used along with the attention layer to capture the temporal relationships between

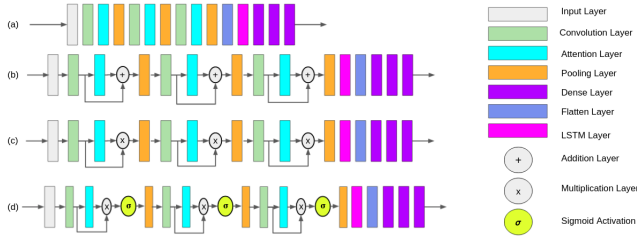


Fig. 3: Feature Network Architectures with attention layers. (a) (`arch:0`) attention layer (cyan) is placed after each convolutional layer (green), (b) (`arch:1`) Output of the attention layer is added to its input before being passed to the next layer: $y = x + \text{Attention}(x)$. (c) (`arch:2`) Output of the attention layer is multiplied to its input: $y = x * \text{Attention}(x)$ (d) (`arch:3`) the output of architecture (c) is passed through a sigmoid activation function: $y = \sigma(x * \text{Attention}(x))$.

the frames. The effect of attention layers on learning performance of RL algorithms is discussed in the next section.

IV. EXPERIMENTS

The details of experiments carried out and the analysis of results are presented in this section as described below.

A. Software and Hardware Configurations

The algorithms were implemented using Python 3.7 and Tensorflow 2.4 on Ubuntu 20.04 GNU/Linux operating system. The source codes are made available publicly on github [25] for the convenience of readers and to ensure reproducibility of results. The plots were drawn using wandb machine learning platform [6]. The pre-built simulation environments available with Pybullet [37] were used for generating the results presented in this paper. The problem environments that are included this study are `KukaDiverseObjectEnv` and `RaceCarZEDGymEnv`. In these environments, the state observation is available in the form of RGB images and the action space is continuous, thereby making them suitable for this study which concerns itself with the hand-eye coordination or vision-based robotics problem. Each run of the program takes about 4-7 hours on a GeForce RTX 2060 GPU machine with about 6 GB of dedicated video RAM. Various hyper-parameters used for different algorithms is shown in Table I. Each season corresponds to 1024 time-steps which is approximately about 140 episodes with 7-8 steps per episode in case of Kuka environment. This is also the length of trajectory segment (denoted by $|\mathcal{D}|$) which is used for on-policy training algorithms such as PPO. Each of the algorithm is executed at least for 5 runs with random seed initialization to generate the statistical plots. The attention and LSTM layers are implemented using Keras APIs.

Parameters	Value
Replay Buffer Size $ \mathcal{B} $	20,000
Batch size	128
Training epochs	20
Trajectory Length (On-policy buffer) $ \mathcal{D} $	1024
Discount factor γ	0.995
Learning rate η	0.002
Input stack size	7
Polyak averaging factor τ	0.995
Clip Factor in PPO ϵ	0.2
Discount factor in GAE λ	0.7
Entropy Coefficient in SAC α	0.2

TABLE I: Hyper-parameters used for different RL algorithms.

B. Benchmarking of RL Algorithms

The performance of four state-of-the-art RL algorithms namely, Soft Actor Critic (SAC) [16], Proximal Policy Optimization (PPO) [43], Interpolated Policy Gradient (IPG) [15] and Hindsight Experience Replay (HER) [1] is compared for two OpenAI/Gym simulation problem environments, namely, `KukaDiverseObjectEnv` and `RaceCarZEDGymEnv` respectively. The outcome is shown in Figures 4 and 5 respectively. One can observe that IPG provides superior performance compared to SAC and PPO. The HER variant of IPG, called, IPG+HER provides better performance compared to IPG. It is also shown that the performance can be improved further by using attention layers. The results are consistent for both the example problems.

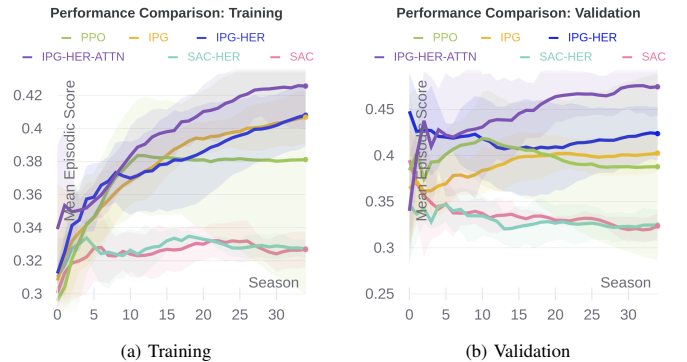


Fig. 4: Performance Comparison of various RL methods for `KukaDiverseObject` Environment. The mean episodic score average over seasons is shown on the y-axis. Each season corresponds to 1024 time-steps or about 140 episodes. Validation involves computing rewards for 50 episodes with deterministic action policy. The off-policy and on-policy training steps are mapped to seasons for comparison.

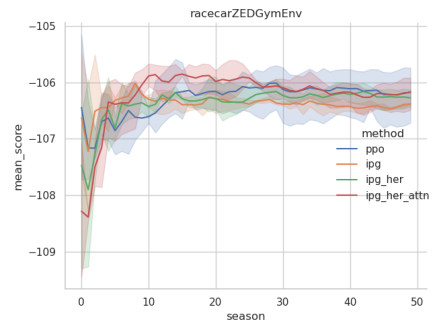


Fig. 5: Performance Comparison of RL algorithms for `RaceCarZEDGymEnv`. The maximum number of steps in an episode is limited to 20. The input images are resized to (40,40,3) before its use in the training. The y-axis shows the mean episodic score against the seasons on x-axis.

C. Effect of Attention on learning performance

Figures 4 and 5 show that it is possible to obtain better learning performance using attention layers. The effect of various attention architectures discussed in Section III-G is shown in Figure 6. It is seen that the architectures `'Luong:2'`, `'Bahdanau:0'`, `'Bahdanau:2'`

provide considerable improvement over the base algorithm (IPG-HER) in case of KukaDiverseObjEnv.

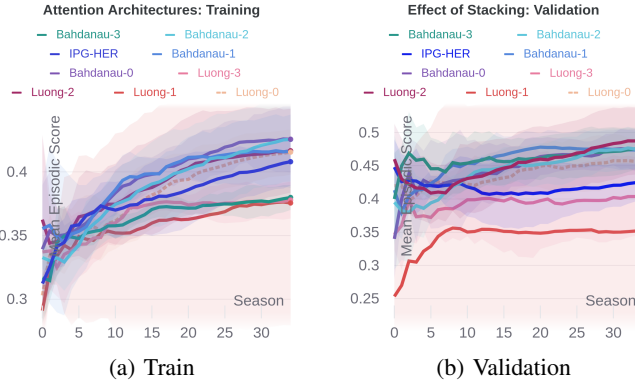


Fig. 6: Effect of attention mechanisms and architectures on the learning performance of IPG-HER algorithm. The IPG-HER algorithm without attention acts as a baseline for comparison (shows in dark blue). Two attention types, namely, Bahdanau and Luong, are considered. Four architectures are shown in Figure 3. Other hyper-parameters are: `her_strategy: 'future'`, `stack_size=1`.

The output of different attention layers is visualized using grad-CAM [44] is shown in Figure 7. The highlighted regions in the image are the areas which were given more importance for computing actions for that particular state.

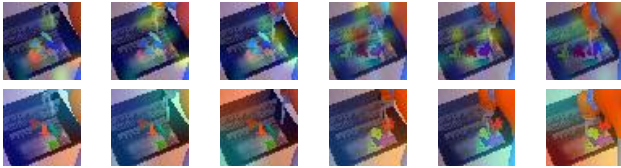


Fig. 7: Gradient Content Activation Map attention Layers. The top row shows the output of the second attention layer and the bottom row shows the output of the outermost attention layer.

D. Effect of HER strategies

The effect of various strategies for selecting intermediate goals on RL performance is shown in Figure 8. It is seen that the ‘future’ strategy provides superior performance compared to other strategies. Further improvement is obtained when the extracted features are used for computing the intermediate rewards for the agent. This is denoted by the letter ‘F’ in the algorithm names mentioned in the legend.

E. Effect of using stacked Frames

The temporal relationships present in the state input can be taken into consideration by stacking the frames together and is known to overcome the partial observability problem in a Markov decision process (MDP) [21] [31]. The effect of using stacked frames on the learning performance is shown in Figure 9. It is observed that stacking itself does not improve the learning performance (blue vs brown curves). However it improves the learning performance when used along with attention and/or LSTM layers. The best performance is obtained when LSTM, Attention and Stacking are used together. It can be concluded that incorporating spatial

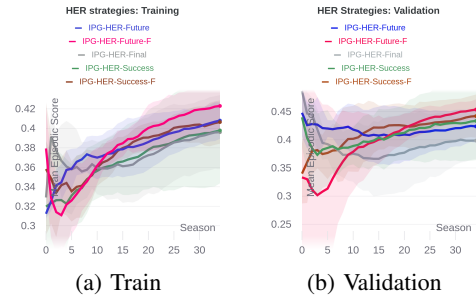


Fig. 8: Effect of goal selection in HER on learning performance. The letter ‘F’ indicates that the L2-distance is computed for the extracted features of the state and the goal images instead of using the raw images.

and temporal attention can improve the performance of RL algorithms.

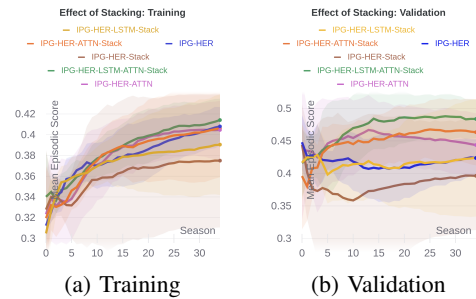


Fig. 9: Effect of Stacking on performance of IPG-HER algorithm for KukaDiverseObjectEnv. It is observed that attention is more effective in improving RL performance with stacked input frames. LSTM is also found to improve the learning performance with stacking. The best performance is obtained by combining attention with LSTM and stacking. Hyper-parameters used are: `attn_arch= Luong:0`, `stack_size=7`, `her_strategy='future'`.

V. CONCLUSION

This paper presents a benchmarking study of some of the state-of-the-art reinforcement learning algorithms for two simulated vision-based robotics problems namely, KukaDiverseObjectEnv and RaceCarZedGymEnv. In both of these two environments, the observation is available in the form of RGB images and the action space is continuous making them suitable for this study. The algorithms considered for benchmarking include Soft Actor Critic (SAC), Proximal Policy Optimization (PPO), Interpolated Policy Gradients (IPG) and Hindsight Experience Replay (HER). A number of strategies are suggested to select intermediate goals required for implementing HER algorithm on these single-goal problem environments. In addition, it is shown that the learning performance of RL algorithms could be enhanced further by applying spatial and temporal attention. To the best of our knowledge such a benchmarking study for these two environments are not available in the literature making it a novel contribution in the field. The future direction would be to implement these algorithms to multi-goal environments with image inputs, which are now becoming available recently. Another direction would be to extend this benchmarking to other robotic problems.

REFERENCES

- [1] M. Andrychowicz, F. Wolski, A. Ray, J. Schneider, R. Fong, P. Welinder, B. McGrew, J. Tobin, P. Abbeel, and W. Zaremba. Hindsight experience replay. *arXiv preprint arXiv:1707.01495*, 2017.
- [2] K. Arulkumaran, M. P. Deisenroth, M. Brundage, and A. A. Bharath. Deep reinforcement learning: A brief survey. *IEEE Signal Processing Magazine*, 34(6):26–38, 2017.
- [3] D. Bahdanau, K. Cho, and Y. Bengio. Neural machine translation by jointly learning to align and translate. *arXiv preprint arXiv:1409.0473*, 2014.
- [4] A. G. Barto. Reinforcement learning and dynamic programming. In *Analysis, Design and Evaluation of Man-Machine Systems 1995*, pages 407–412. Elsevier, 1995.
- [5] Q. Bateux, E. Marchand, J. Leitner, F. Chaumette, and P. Corke. Training deep neural networks for visual servoing. In *2018 IEEE international conference on robotics and automation (ICRA)*, pages 3307–3314. IEEE, 2018.
- [6] L. Biewald. Experiment tracking with weights and biases, 2020. Software available from wandb.com.
- [7] F. Chaumette, S. Hutchinson, and P. Corke. Visual servoing. In *Springer Handbook of Robotics*, pages 841–866. Springer, 2016.
- [8] S. Dankwa and W. Zheng. Twin-delayed ddpq: A deep reinforcement learning technique to model a continuous movement of an intelligent robot agent. In *Proceedings of the 3rd International Conference on Vision, Image and Signal Processing*, pages 1–5, 2019.
- [9] Y. Duan, X. Chen, R. Houthoofd, J. Schulman, and P. Abbeel. Benchmarking deep reinforcement learning for continuous control. In *International conference on machine learning*, pages 1329–1338. PMLR, 2016.
- [10] FetchReach-v1. A multi-goal OpenAI/Gym environment by mujoco. <https://gym.openai.com/envs/FetchReach-v1/>.
- [11] T. Fukuda. *Soft Computing for Intelligent Robotic Systems*. Springer, 1998.
- [12] Q. Gallouédéc, N. Cazin, E. Dellandréa, and L. Chen. Multi-goal reinforcement learning environments for simulated franka emika panda robot. *arXiv preprint arXiv:2106.13687*, 2021.
- [13] I. Grondman, L. Busoniu, G. A. Lopes, and R. Babuska. A survey of actor-critic reinforcement learning: Standard and natural policy gradients. *IEEE Transactions on Systems, Man, and Cybernetics, Part C (Applications and Reviews)*, 42(6):1291–1307, 2012.
- [14] S. Gu, E. Holly, T. Lillicrap, and S. Levine. Deep reinforcement learning for robotic manipulation with asynchronous off-policy updates. In *2017 IEEE international conference on robotics and automation (ICRA)*, pages 3389–3396. IEEE, 2017.
- [15] S. Gu, T. Lillicrap, Z. Ghahramani, R. E. Turner, B. Schölkopf, and S. Levine. Interpolated policy gradient: Merging on-policy and off-policy gradient estimation for deep reinforcement learning. *arXiv preprint arXiv:1706.00387*, 2017.
- [16] T. Haarnoja, A. Zhou, P. Abbeel, and S. Levine. Soft actor-critic: Off-policy maximum entropy deep reinforcement learning with a stochastic actor. In *International conference on machine learning*, pages 1861–1870. PMLR, 2018.
- [17] G. D. Hager, W.-C. Chang, and A. S. Morse. Robot hand-eye coordination based on stereo vision. *IEEE Control Systems Magazine*, 15(1):30–39, 1995.
- [18] S. D. Holcomb, W. K. Porter, S. V. Ault, G. Mao, and J. Wang. Overview on deepmind and its alphago zero ai. In *Proceedings of the 2018 international conference on big data and education*, pages 67–71, 2018.
- [19] S. Iqbal and F. Sha. Actor-attention-critic for multi-agent reinforcement learning. In *International Conference on Machine Learning*, pages 2961–2970. PMLR, 2019.
- [20] S. Joshi, S. Kumar, and F. Sahin. Robotic grasping using deep reinforcement learning. In *2020 IEEE 16th International Conference on Automation Science and Engineering (CASE)*, pages 1461–1466. IEEE, 2020.
- [21] S. Kapturowski, G. Ostrovski, J. Quan, R. Munos, and W. Dabney. Recurrent experience replay in distributed reinforcement learning. In *International conference on learning representations*, 2018.
- [22] S. Khan, M. Naseer, M. Hayat, S. W. Zamir, F. S. Khan, and M. Shah. Transformers in vision: A survey. *arXiv preprint arXiv:2101.01169*, 2021.
- [23] V. R. Konda and J. N. Tsitsiklis. Actor-critic algorithms. In *Advances in neural information processing systems*, pages 1008–1014, 2000.
- [24] P. P. Kumar and L. Behera. Visual servoing of redundant manipulator with jacobian matrix estimation using self-organizing map. *Robotics and Autonomous Systems*, 58(8):978–990, 2010.
- [25] S. Kumar. Benchmarking of deep reinforcement learning algorithms. <https://github.com/swagatk/RL-Projects-SK.git>.
- [26] A. X. Lee, S. Levine, and P. Abbeel. Learning visual servoing with deep features and fitted q-iteration. *arXiv preprint arXiv:1703.11000*, 2017.
- [27] Y. Li and J. Košečka. Learning view and target invariant visual servoing for navigation. In *2020 IEEE International Conference on Robotics and Automation (ICRA)*, pages 658–664. IEEE, 2020.
- [28] T. P. Lillicrap, J. J. Hunt, A. Pritzel, N. Heess, T. Erez, Y. Tassa, D. Silver, and D. Wierstra. Continuous control with deep reinforcement learning. *arXiv preprint arXiv:1509.02971*, 2015.
- [29] M.-T. Luong, H. Pham, and C. D. Manning. Effective approaches to attention-based neural machine translation. *arXiv preprint arXiv:1508.04025*, 2015.
- [30] A. R. Mahmood, D. Korenkevych, G. Vasan, W. Ma, and J. Bergstra. Benchmarking reinforcement learning algorithms on real-world robots. In *Conference on robot learning*, pages 561–591. PMLR, 2018.
- [31] A. Manchin, E. Abbasnejad, and A. van den Hengel. Reinforcement learning with attention that works: A self-supervised approach. In *International Conference on Neural Information Processing*, pages 223–230. Springer, 2019.
- [32] V. Mnih, K. Kavukcuoglu, D. Silver, A. Graves, I. Antonoglou, D. Wierstra, and M. Riedmiller. Playing atari with deep reinforcement learning. *arXiv preprint arXiv:1312.5602*, 2013.
- [33] MuJoCo. Advanced physics simulation. <http://www.mujoco.org/>.
- [34] H. Nguyen and H. La. Review of deep reinforcement learning for robot manipulation. In *2019 Third IEEE International Conference on Robotic Computing (IRC)*, pages 590–595. IEEE, 2019.
- [35] M. Plappert, M. Andrychowicz, A. Ray, B. McGrew, B. Baker, G. Powell, J. Schneider, J. Tobin, M. Chociej, P. Welinder, et al. Multi-goal reinforcement learning: Challenging robotics environments and request for research. *arXiv preprint arXiv:1802.09464*, 2018.
- [36] B. T. Polyak and A. B. Juditsky. Acceleration of stochastic approximation by averaging. *SIAM journal on control and optimization*, 30(4):838–855, 1992.
- [37] PyBullet. Bullet real-time physics simulation. <https://pybullet.org/wordpress/>.
- [38] D. Quillen, E. Jang, O. Nachum, C. Finn, J. Ibarz, and S. Levine. Deep reinforcement learning for vision-based robotic grasping: A simulated comparative evaluation of off-policy methods. In *2018 IEEE International Conference on Robotics and Automation (ICRA)*, pages 6284–6291. IEEE, 2018.
- [39] S. Salter, D. Rao, M. Wulfmeier, R. Hadsell, and I. Posner. Attention-privileged reinforcement learning. *arXiv preprint arXiv:1911.08363*, 2019.
- [40] A. Saxena, H. Pandya, G. Kumar, A. Gaud, and K. M. Krishna. Exploring convolutional networks for end-to-end visual servoing. In *2017 IEEE International Conference on Robotics and Automation (ICRA)*, pages 3817–3823. IEEE, 2017.
- [41] J. Schulman, S. Levine, P. Abbeel, M. Jordan, and P. Moritz. Trust region policy optimization. In *International conference on machine learning*, pages 1889–1897. PMLR, 2015.
- [42] J. Schulman, P. Moritz, S. Levine, M. Jordan, and P. Abbeel. High-dimensional continuous control using generalized advantage estimation. *arXiv preprint arXiv:1506.02438*, 2015.
- [43] J. Schulman, F. Wolski, P. Dhariwal, A. Radford, and O. Klimov. Proximal policy optimization algorithms. *arXiv preprint arXiv:1707.06347*, 2017.
- [44] R. R. Selvaraju, M. Cogswell, A. Das, R. Vedantam, D. Parikh, and D. Batra. Grad-cam: Visual explanations from deep networks via gradient-based localization. In *Proceedings of the IEEE international conference on computer vision*, pages 618–626, 2017.
- [45] M. Sewak. Deep q network (dqn), double dqn, and dueling dqn. In *Deep Reinforcement Learning*, pages 95–108. Springer, 2019.
- [46] I. H. Suh and T. W. Kim. Fuzzy membership function based neural networks with applications to the visual servoing of robot manipulators. *IEEE Transactions on Fuzzy Systems*, 2(3):203–220, 1994.
- [47] R. S. Sutton and A. G. Barto. *Reinforcement learning: An introduction*. MIT press, 2018.
- [48] H. Van Hasselt, A. Guez, and D. Silver. Deep reinforcement learning with double q-learning. In *Proceedings of the AAAI Conference on Artificial Intelligence*, volume 30, 2016.
- [49] A. Vaswani, N. Shazeer, N. Parmar, J. Uszkoreit, L. Jones, A. N. Gomez, Ł. Kaiser, and I. Polosukhin. Attention is all you need. In *Advances in neural information processing systems*, pages 5998–6008, 2017.

- [50] P. Yue, J. Xin, H. Zhao, D. Liu, M. Shan, and J. Zhang. Experimental research on deep reinforcement learning in autonomous navigation of mobile robot. In *2019 14th IEEE Conference on Industrial Electronics and Applications (ICIEA)*, pages 1612–1616. IEEE, 2019.